Proceedings of the SEM International Conference & Exposition on Experimental and Applied Mechanics June 11-12, 2012 Costa Mesa, California USA

High Strain Rate Characteristics of Fiber Bragg Grating Strain sensors

Wun-Jheng Lin[1], Liren Tsai[1], Cia-Chin Chiang[1], Shih-Han Wang[2]
[1]National Kaohsiung University of Applied Sciences, Graduate Institute of Mechanical and Precision Engineering, Chien Kung Campus 415 Chien Kung Road, Kaohsiung 807, Taiwan, R.O.C.
[2]I-Shou University, Department of Chemical Engineering & Institute of Biotechnology and Chemical Engineering, No.1, Sec. 1, Xuecheng Rd., Dashu Dist., Kaohsiung City 840, Taiwan R.O.C.
Tel: (07)3814526 ext. 5323, Email: liren@cc.kuas.edu.tw

Abstract

Fiber Bragg Grating sensors (FBGs) have been utilized in various engineering fields because of their lightweight and good environment tolerance. In this research, FBG strain sensors were embedded inside carbon fiber reinforced polymer composites (CFRP) to study the FBG wave spectrums at high strain rate. The FBG embedded CFRP specimens were machined to dog-bone shape and a foil strain gauge was attached at its gauge section. The dynamic response of FBG sensors were then examined using split Hopkinson tension bar (SHTB). By comparing the strain measurements from FBGs, foil gauges, and SHTB measurements, the high strain rate behavior of FBG strain sensors was able to be explored at strain rates between 130 s^{-1} to 2100 s^{-1}.

Keyword: SHTB, dynamic responses, Fiber Bragg Grating sensor

1. Introduction

Today, various researchers forced on composites material in the past decades, because of its excellent characteristics in engineering applications such as low density, high thermal conductivity rate, and high elastic strength [1]. CFRP was widely utilized in many engineering fields, it is composed of polymer matrix with carbon fibers, and CFRPs were usually composed of 10~70% of carbon fibers [2-3]. Polymer matrix provides support to cohere with each carbon fiber and increased the toughness and strength of the composite. The matrix could also prevent the environmental erosion and oxidation [3-4]. Meanwhile, optical fiber has evolved in many technology fields in modern telecommunication system and photonics [5]. Optical fiber grating was found in 1978s, and flow production in 1993s [6]. When periodic gratings were applied on the optical fiber, the fiber possesses fiber Bragg grating characteristics. When FBG was subjected to a perturb, the refractive index would change hence resulted in a coupling phenomenon, i.e. when external force acts on the optical fiber, the grating structure of FBG would affect the light signal transmit, and the applied force or strain of the optical fiber could be determined [6].

FBG sensors were very suitable for measuring in situ strain behavior of composite materials. K.S.C. Kuang and R. Kenny et al., studied various composite materials using embedded FBG strain sensors, and the results showed that FBGs exhibit linearly strain measurement response under quasi-static tension tests [7]. Y. Okabe and S. Yashiro et al. found that when embedding FBG sensors in polymer matrix, the residual stress would occur [8]. In this research, we embedded the long period fiber Bragg grating into the carbon fiber composite material, and the dynamic response of this embedded FBG sensor under shock loading is examined. Moreover, the specimen was attached foil strain gauge to measure the surface strain of each specimen. As the result, the strain history and sensitive of FBG were discussed.

2. Method and Material

2.1 SHTB

A split Hopkinson tensile bar facility at Kaohsiung University of Applied Sciences was utilized in this research. The SHTB setup included striker, incident bar, transmission bar and momentum trap bar, and the bar lengths were 400mm, 2000mm, 1000mm and 400mm, respectively. The semi-conductor strain gauges were utilized to measure the wave signal. While elastic wave propagated through incident bar, the elastic wave had two types. One was passed through to specimen, and the other was reflected back to incident bar, and by using one dimensional wave theory, the resultant stress vs. strain curves of CFRPs were determined [9-12].

2.2 Fiber Bragg Grating sensor

The FBG sensing system utilized in this research consists of photodiode (PD), light source, optical tunable filter and couple, as show in figure 1(a). The optical fiber were expanded under tensile forces, then its light passes through core grating (likes Bessel function) section and its wavelength were displaced. After that, the signal were recorded and analyzed, its signal were compared with strain signal of strain gauge to calculate the sensitivity coefficients. The L/W ratios were controlled between 2-4 rates [13] and FBG sensors of data and foil strain gauges were acquired through static testing, and each FBG was calculated to ensure its high accuracy.

2.2.1 Principal of optical fiber gratings

Theory of grating was defined in geometrical optics of diffraction: from periodic slit structures. While light sources emitted in a transverse slit plane, it resulted in a shade of diffractive stripe. And this periodic slit structure was called grating structure [6, 14].

$$n \sin \theta_2 = n \sin \theta_1 + m \frac{\lambda}{\Lambda} \tag{1}$$

In Eq. (1), n is the refractive index of medium, λ is the wavelength, Λ is the grating of period, m is the diffraction of order, θ_1 is the light of incident angle and θ_2 is the diffractive angle for -1 order.

In figure 1(b), optical fiber grating structure was engraved onto optical fiber. The light emitted in optical fiber and resulted in diffractive phenomenon. The propagation constant was defined given by [6, 14]:

$$\beta = \left(\frac{2\pi}{\lambda} \right) n_{eff} \tag{2}$$

2.2.2 Theory of Fiber Bragg Grating

Fiber Bragg Grating were called reflective fiber grating, furthermore, it utilized reflection to monitor light reflective spectrums. Forward incident light were coupled with backward reflective light, and it was reflective via grating section. The Fiber Bragg Grating equation was given by [6, 14]:

$$\lambda = 2 n_{eff} \Lambda \tag{3}$$

The λ is the Bragg wavelength, n_{eff} is the effective reflective index and Λ is the periodic grating [6, 14].

2.3 Specimen preparation

In this study, the material of pre-preg was combined with 63% fibrous and 37% matrix. The width and thickness of specimens were designed as 4mm and 2mm, and its layers were folded up with [0/45/0/-45/0]s. In the specimen curing process, it was cured under a vacuum situation, and was heated to 240℃. The pre-pregs were air-cooled until its temperature decreased to room temperature. Then each specimen was machined to dog-bone shape by water-jet cutting.

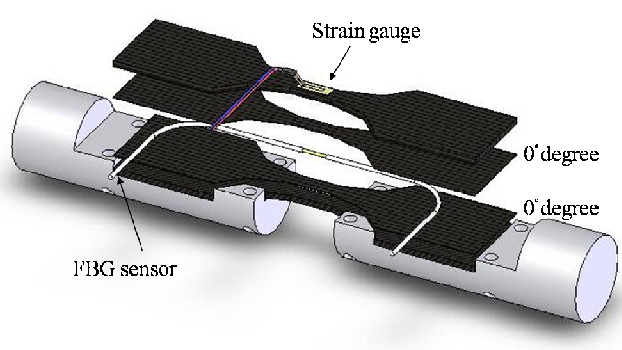

(a)

Proceedings of the SEM International Conference & Exposition on Experimental and Applied Mechanics June 11-12, 2012 Costa Mesa, California USA

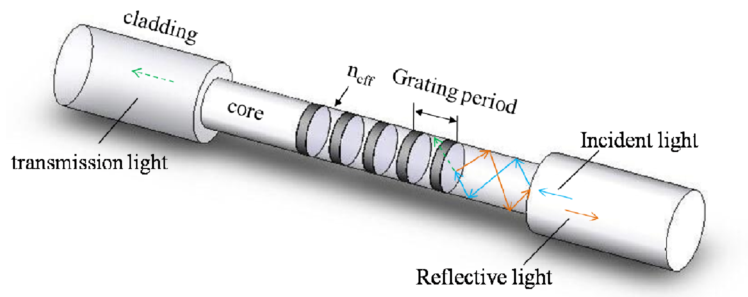

(b)

Fig. 1 schematic diagram of (a) specimen [0/45/0/-45/0]s, and (b) Fiber Bragg Grating sensor of principle

(a)

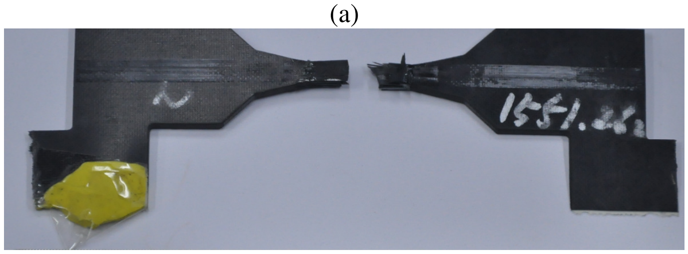

(b)

Fig. 2 The specimen of (a) and (b) CFRP were before and after dynamic loading

3. Result and discussion

In this research, Split Hopkinson Tensile Bar (SHTB) was utilized to study the dynamic behavior of FBG and materials. The specimens were fixed in incident bar and transmission bar, and then the air pressure projected the impact bar to strike the incident bar. The strain waves propagated through the specimen, between incident bar and transmitted bar. The part of stress wave was reflected to incident bar because there were impedance mismatch. In order to understand the FBG sensor wave spectrum under dynamic situation, it FBGs were embedded inside CFRP materials, and foil strain gauges were attached on each specimen. In the dynamic responses of CFRP, stress-strain curve, FBG sensors and strain gauges measurements were presented in fig. 5 (a) (b) (c), respectively. Young's modulus and yield stress were shown in table 1.

Table 1 Mechanical property of CFRP under high strain rate

Strain rate (s^{-1})	Young's modulus (GPa)	Yield stress (MPa)
135	158.7	455.3
323	275.6	953.5
492	223.6	1333.8
721	147.3	1445.9
983.5	165.5	1833

Strain rates between $135s^{-1}$~$983.5s^{-1}$ were applied to examine the dynamic response of FBGs and CFRPs. Young's modulus was direct proportional to strain rates. The specimens exhibit tensile fracture at the neck of specimen under high stain rate loadings. According to scanning electron microscopy, as shown in fig. 3, after dynamic loading, fibers inside specimen were cracked at certain degrees. After shock loading the FBG sensors were cracked, it's conceivable to understand the brittle material in a destroyed situation.

Young's modulus of CFRP in this research have shown the results of 158.7 GPa at strain rate $135s^{-1}$ and 165.5 GPa at strain rate $983.5s^{-1}$, yield stress of CFRP was 455.3 MPa at strain rate 135^{-1} and 1833 MPa at strain rate $983.5s^{-1}$, respectively. When comparing the recorded strain signal from FBG and surface strain gauge, as shown in fig. 4 (b), FBG sensor exhibit higher precision.

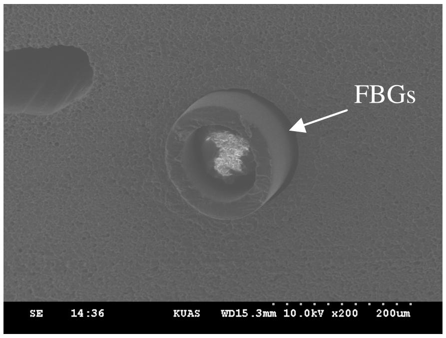

(a)

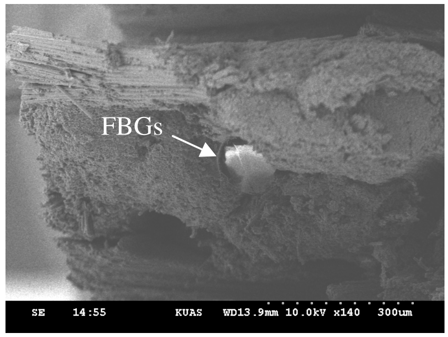

(b)

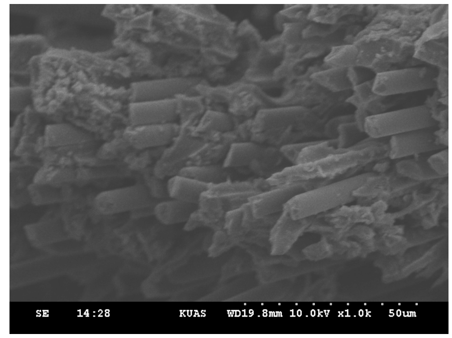

(c)

Fig. 3 (a) Normal FBG sensor surfaced, (b) FBG sensor, and (c) CFRP was surfaced feature under high-speed loading.

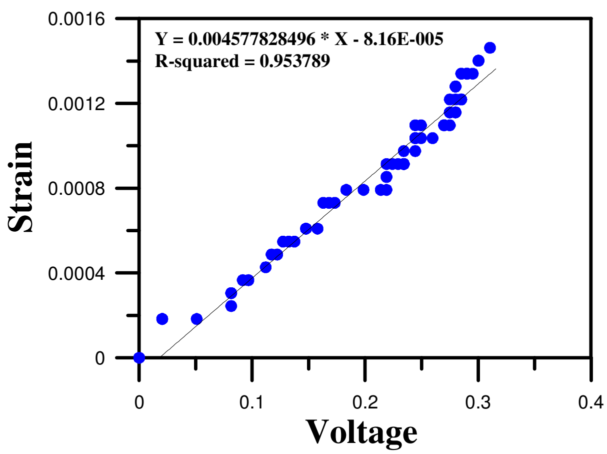

(a)

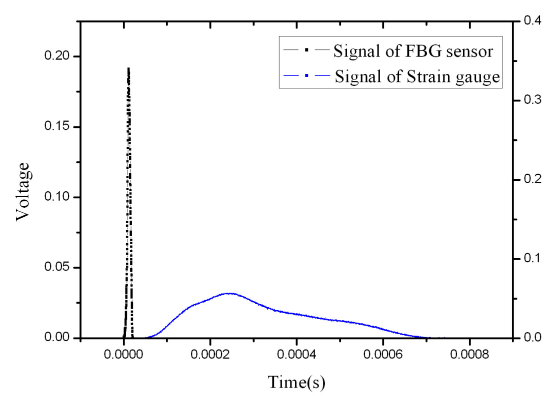

(b)

Fig. 4 (a) the FBGs of date and strain of value were calculated for linear equations, (b) Signal of FBG sensor and Strain gauge under high strain rate $492s^{-1}$

In fig. 4 (a), the gauge factors of FBG were calibrated using a MTS tensile test before each experiment. Figure 4(b) shows the raw data of both FBG and surface strain gauge. From this voltage vs. time profile, it is quite clear that the FBG strain sensor has higher sensitivity and quicker response time. CFRP specimen was strain measured by FBG sensor and foil strain gauge increased sharply under shock loadings. The strain vs. time as well as stress vs. strain curves were presented in figure 5. In figure 5 (a) and 5(b), strain vs. time profile of FBGs and surface strain gauges were presented, respectively. At lower strain rate conditions, both FBG and strain gauge curves exhibit J-shape curve feature, however, when strain rates increased to more than 700 s^{-1}, strain gauge signals started to vibrate severely at higher strain range. As shown in fig. 5 (c), the SHTB results showed clear yield strength increments with increasing strain rates between 135 $s^{-1}$to 982.5 s^{-1}.

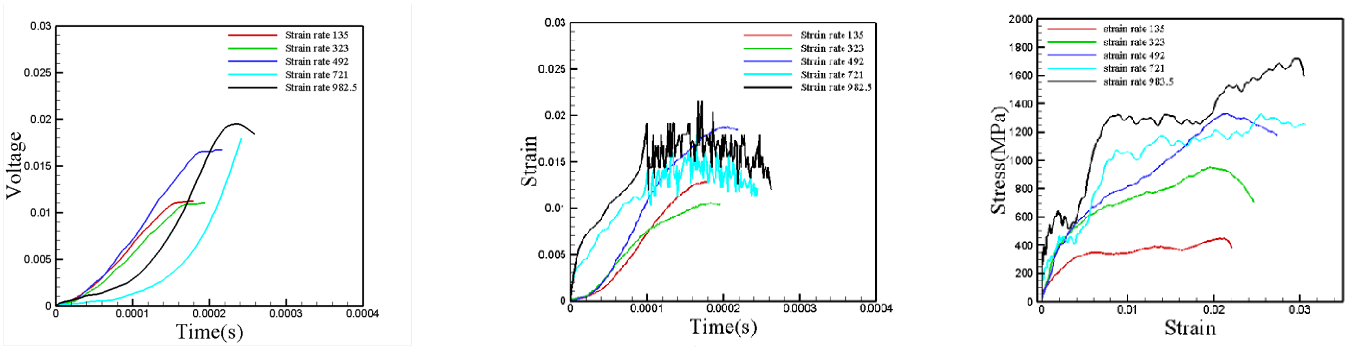

(a) (b) (c)

Fig. 5 (a) FBGs and (b) strain gauge of strain-time curve under strain rate 135 s^{-1} to 982.5 s^{-1}, (c) the stress-strain curve of CFRP under strain rate 135 s^{-1} to 982.5s^{-1}

4. Conclusion

The stresses of specimen were direct proportional to strain rate. The results of SHTB measures and FBG sensors and foil strain gauges were investigated under dynamic loading from 135s^{-1} to 983.5s^{-1}. FBG sensors were more environment tolerance than foil strain gauges, and in addition, FBG sensors were embedded inside materials and monitored the material strain conditions inside composite materials.

Acknowledgments

This study was supported from National sciences council, and plan of no. NSC-99-2221-E-151-014 National Kaohsiung University of applied sciences in Taiwan. It's deeply appreciated Professor L.R. Tsai and Professor C.C. Chiang to help in this research.

Reference

[1] S.K. Suk, S.R. Bhowmik, T. Windhorst, G. Blount, "Carbon-carbon Composites: a Summary of Recent Developments and Applications," Materials & Design, Vol. 18, No. 1, pp.11–15, 1997.
[2] H.C. Lee, "The influences of residual stress in epoxy carbon-fiber composites under high strain-rate. " Master Thesis, National Kaohsiung University of Applied Sciences, Kaohsiung Taiwan. 2010
[3] G.R. Devi, K.R. Rao, "Carbon-Carbon Composites -An Overview," Defence Science Journal, Vol. 43,No 4, pp. 369-383, 1993
[4] J.M. Lifshitz, H. Leber, "Respond of fiber-reinforced polymers to high strain-rate loading interlaminar tension and combined tension/shear," Composites Science and Technology, Vol. 58, No. 6, pp. 987-996, 1998.
[5] R. Kashyap, "Fiber Bragg Grating." Photon design, Elsevier Inc, pp.596, ISBN 978-0-12-372579-0, 2010
[6] J. Liou, "Curing monitor of the composite material by optical fiber grating sensors." Master Thesis, National Kaohsiung University of Applied Sciences, Kaohsiung Taiwan. 2010
[7] K.S.C. Kuang, R. Kennyb, M.P. Whelanb, W.J. Cantwell, P.R. Chalker, "Embedded fibre Bragg grating sensors in advanced composite materials." Composites Science and Technology 61, Vol.61, No.10, pp. 1379–1387, 2001.
[8] Y. Okabe, S. Yashiro, T. Kosaka and N. Takeda, "Detection of transverse cracks in CFRP composites using embedded fiber Bragg grating sensors." Vol.9, No.6, pp. 832–838, 2000.
[9] L.J. Griffiths, D.J. Martin, "A study of the dynamic behaviour of a carbon-fibre composite using the split Hopkinson pressure bar," Journal of Physics D: Applied Physics, Vol. 7, No.17, pp.2329-2341, 1974.
[10] J. Harding and L.M. Welsh, "A tensile testing technique for fibre-reinforced composites at impact rates of strain," Journal of Materials Science, Vol.18, No.6, pp. 1810–1826, 1983.
[11] ASM Int, Mechanical Testing and Evaluation, ASM Handbook, ASM Int, Materials Park OH, Vol. 8, 2000.
[12] H. Kolsky, "An Investigation of the Mechanical Properties of Materials at very High Rates of Loading," Proceedings of the Physical Society. Section B, Vol.62, No.11, pp. 676–700, 1949.
[13] X. Yang, A. Nanni, L. Dharani, "Effect of fiber misalignment on FRP laminates and strengthend concrete beams," Structural Faults and Repair, pp.4-6, 2001.
[14] L.W. Jhong, "The research of Fiber Gratings theory computation and Actual Formation." Master thesis, Chung Cheng Institute of Technology National Defense University, Taiwan, 1999.